INSTITUTE OF PHYSICS PUBLISHING JOURNAL OF PHYSICS: CONDENSED MATTER

J. Phys.: Condens. Matter **14** (2002) 9275–9283 PII: S0953-8984(02)36382-3

Viscosity of ultra-thin water films confined between hydrophobic or hydrophilic surfaces

Uri Raviv[1], **Suzanne Giasson**[2], **Joseph Frey**[1,4] **and Jacob Klein**[1,3,5]

[1] Department of Materials and Interfaces, Weizmann Institute of Science, Rehovot 76100, Israel
[2] Department of Chemical Engineering and CERSIM, Laval University, Québec, Qc, Canada G1K 7P4
[3] Physical and Theoretical Chemistry Laboratory, Oxford University, South Parks Road, Oxford OX1 3QZ, UK

Received 30 April 2002, in final form 6 June 2002
Published 27 September 2002
Online at stacks.iop.org/JPhysCM/14/9275

Abstract

A surface force balance has been used to investigate the viscosity of salt-free (conductivity) water confined between hydrophilic and between hydrophobic surfaces. We examine the process of jump-in, across the last few nanometres of thin water films, to adhesive contact between the surfaces. We analyse the flow of water out of the gap under slip and no-slip boundary conditions at the confining surfaces. In both cases we find that the effective viscosity of water remains comparable to its bulk value even when it is confined to sub-nanometre thin films.

1. Introduction

The properties of water in the vicinity of surfaces and under confinement have been studied extensively because of their importance in colloidal dispersions and tribology, and particularly because of their relevance to a quantitative understanding of many processes in biological systems [1–9]. The fluidity of water in confined geometries and its molecular mobility in pores and slits has been extensively studied using a variety of indirect methods [2, 5, 10–12]. Earlier studies where liquid flow is measured directly suggest that the viscosity of aqueous electrolytes confined to films of thickness greater than some 2–3 nm remains close to that of the bulk [13, 14].

In a recent study we have shown that, in contrast to non-associating liquids, whose viscosity diverges when confined to molecularly thin films [15, 16], the effective viscosity η_{eff} of water remains close to its bulk value η_{bulk} (within a factor of three either side of η_{bulk}) even when it is confined between two (hydrophilic) mica surfaces to films in the thickness range 3.5 ± 1 to 0.0 ± 0.4 nm [17]. Two observations supported this conclusion. The first was that, when

[4] Current address: Melville Laboratory for Polymer Synthesis, Department of Chemistry, University of Cambridge, Lensfield Rd, Cambridge CB2 1EW, UK.
[5] Author to whom any correspondence should be addressed.

the films were sheared, the shear stresses maintained by these films, over the shear rates used, were immeasurably low (within our resolution), thereby setting an upper limit on η_{eff}, of about $100\eta_{bulk}$. The second and more stringent limit on the effective viscosity was obtained from the analysis of the time it takes for the two mica surfaces to jump from a separation distance D of 3.5 ± 1 nm into a flat adhesive contact at $D = 0.0 \pm 0.4$ nm due to the van der Waals (vdW) attractive forces between the surfaces across water. The underlying assumption in this analysis was that, as mica surfaces are hydrophilic, there is no slippage of liquid on the solid surfaces. Dynamic surface force investigations [13, 14] and other studies [18] underpin the validity of this assumption.

Recently it has been suggested that slippage may occur on poorly wetted or lyophobic surfaces [18–21]. In the present paper the viscosity of water when confined between two hydrophobic or two hydrophilic surfaces is studied. The flow of water out of the gap is analysed, allowing arbitrary slippage of liquid (over an appropriate range) to occur at the surface. The no-slip boundary condition in the case of hydrophilic surfaces is thus examined and compared with the case of hydrophobic surfaces, which allow water slippage at the surface. Although we do not expect to have slippage of water on the hydrophilic mica surfaces [13, 14], it is still of interest to examine the possibility that slippage occurs to some extent and to estimate its effect on the effective viscosity obtained by the jump time analysis. In addition, experimental results are presented on the jump to contact of two hydrophobized mica surfaces across salt-free water, which are analysed to extract the effective viscosity of the confined liquid.

2. Experimental details

The normal forces $F_n(D)$ between two opposing curved mica surfaces (of mean radius R) in a crossed-cylinder configuration, as a function of their closest separation D, was directly measured using a surface force balance, SFB, for which detailed experimental procedures have been described elsewhere [22, 23]. Multiple-beam interference allows the distance between the mica surfaces, which are silvered on their back sides, to be measured with resolution of $\pm$0.2–0.3 nm and their contact geometry (including R) to be determined from the shape of the interference fringes. Changes ΔF_n in the normal force are determined (to within $\pm$100 nN) directly from the bending ΔD of the springs, as $\Delta F_n = K_n \Delta D$, where $K_n = 150$ N m^{-1} is the spring constant.

Water purification

Tap water treated with activated charcoal was passed through a Millipore purification system (RiOs^{TM} followed by a Milli-Q^{TM} gradient stage), yielding water with specific resistivity $>$18.2 MΩ and total organic content $<$4 ppb.

Stearic trimethylammonium iodide (designated STAI: $CH_3(CH_2)_{17}N^+$ $(CH_3)_3I^-$) was prepared according to known methods [24, 25]. The stoichiometrically pure and monodispersed surfactant was crystallized twice from methanol–acetone mixture and an NMR analysis confirmed the elemental composition. A water droplet on an STAI-coated mica surface showed an advancing contact angle of 85°, in agreement with earlier observations [25].

3. Results

Highly purified water (conductivity water) was introduced between curved mica surfaces in the SFB. $F_n(D)$ profiles were then measured and are shown in figure 1. They reveal the long-ranged repulsion associated with the presence of charge on the mica surfaces, arising from the

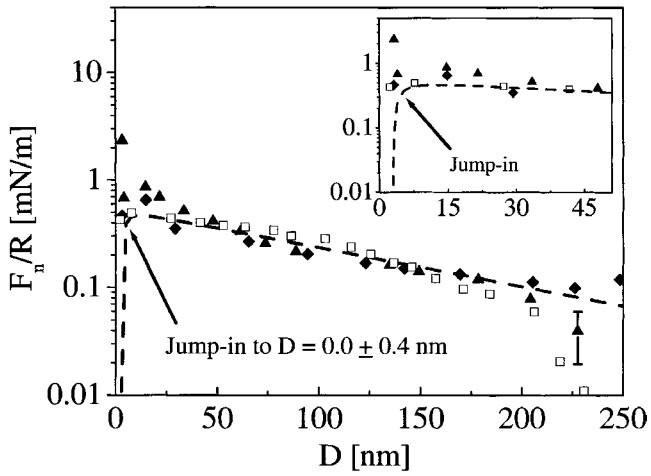

Figure 1. Force (F_n/R) versus distance (D) profile between curved mica surfaces (mean radius of curvature $R \approx 1$ cm) across conductivity water at 23 ± 1 °C. The broken line corresponds to a DLVO expression, $F/R = 128\pi C k_B T \kappa^{-1} \tanh^2(e\psi_0/4k_BT) \exp(-\kappa D) - A/6D^2$, with a Debye length κ^{-1} of 120 ± 20 nm, corresponding to $C = (6.4 \pm 1) \times 10^{-6}$ M 1:1 salt concentration; an effective (large-separation) surface potential ψ_0 of 130 ± 20 mV and a Hamaker constant $A = 2 \times 10^{-20}$ J. Data adapted from [17, 37].

loss of potassium ions to solution. In agreement with earlier work [26], the surfaces jump from separations $D = D_j = 3.5 \pm 1$ nm into flat adhesive contact, $D = D_0 = 0.0 \pm 0.4$ nm (since the size of a water molecule is roughly 0.25 nm, the presence of, at most, one monolayer of water per mica surface following adhesive contact cannot be ruled out within our resolution). The spontaneous inward motion occurs in a single monotonic jump from D_j to D_0 and its duration is estimated as 0.2–0.5 s. It is driven by vdW attraction between the surfaces overcoming the double layer and is due to an instability expected whenever $|(\partial F_n/\partial D)| > K_n$, where K_n is the constant of the normal spring.

The surfaces were then taken out, coated with STAI, as described in detail elsewhere [25, 27], remounted into the SFB and the cell was filled with conductivity water. $F_n(D)$ profiles measured during a first or a second approach are shown in figure 2. The absence of long-ranged interactions (at $D > 50$ nm) is due to charge cancellation at the mica surfaces, arising from condensation of the positive ionic end groups ($(CH_3)_3N^+$) over most of the ionizable lattice sites [28, 29], thereby reducing the surface charge density and consequently the long-ranged double layer repulsive forces. In the case where the STAI layers neutralized nearly all the lattice sites (i.e. the STAI layers exhibited few if any defects), no repulsive forces could be detected (open symbols in figure 2), and attractive hydrophobic forces were detected already at $D = 33 \pm 1$ nm, in agreement with earlier studies (though a certain variability in the range of attractive forces range has been observed [30–36]). The set of data indicated with solid symbols shows short-ranged double-layer repulsive forces due to residual surface charge, associated with slight imperfections in the STAI layers arising from small variations in the hydrophobization procedure (e.g. in the rate of withdrawal of the surfaces from the STAI solution [27]). At $D = D_j^{STAI} = 11 \pm 2$ nm the two STAI-coated surfaces jump into a flat adhesive contact at $D = D_0^{STAI} = 0.7 \pm 0.3$ nm, in agreement with earlier observations [29]. The spontaneous inward motion, which occurs in a single monotonic jump from D_j^{STAI} to D_0^{STAI}, is driven by hydrophobic attraction and the vdW force, and its duration is estimated at less than about 0.5 s.

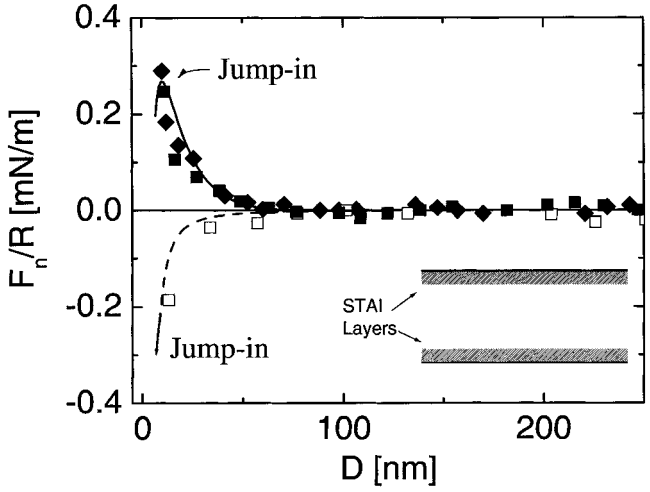

Figure 2. Normalized $F_n(D)$ profiles between hydrophobized (STAI-coated) mica surfaces in conductivity water. Results shown are from two different sets of experiments. The weak short-ranged repulsion prior to jump into contact in one of the profiles (solid symbols) is due to residual charge on the hydrophobized mica surfaces arising from small imperfections in the STAI layers as described in the text. Squares indicate the forces on first approach in the two different experiments. Diamonds indicate the forces on second approach measured following the first approach indicated with solid squares. The solid curve is a fit of data from the experiment indicated with solid symbols to the DLVO expression (figure 1 caption), using a vdW-like expression to approximate the hydrophobic attraction, with $A = A_{eff} = 10^{-19}$ J as an effective Hamaker constant (see text). From the far-field fit we obtained a Debye length of 13 ± 1 nm, and surface potential of 39 ± 5 mV. The broken curve is given by a vdW-like expression: $F_n(D) = -A_{eff}R/6D^2$. For both experiments, at $D = D_j^{STAI} = 11 \pm 2$ nm the two STAI-coated surfaces jump into a flat adhesive contact at $D_0^{STAI} = 0.7 \pm 0.3$ nm.

The jump distance D_j^{STAI} is expected to be the value at the instability point $|(\partial F/\partial D)| = K_n$ where F is the force between the hydrophobic surfaces. We may approximate the form of this hydrophobic attraction by using an expression for a vdW attractive force with an effective Hamaker constant [37][6], $A_{eff} = 10^{-19}$ J. This value is significantly higher than the maximum possible theoretical value for the vdW interaction of two hydrocarbon-coated mica surfaces [29], $A = 1.5 \times 10^{-20}$ J (for which a jump distance of about 7 nm might be expected), and suggests the hydrophobic interaction is the dominant one. When the surface charge density was almost exactly neutralized by the STAI layers and no double-layer forces were measured (open symbols in figure 2), the magnitude and form of the $F_n(D)$ profile could nonetheless be reasonably depicted by a vdW-like expression $F_{\rm vdW} = A_{eff}R/6D^2$, using A_{eff} as Hamaker constant (broken curve in figure 2). We stress that this is intended mainly to provide a reasonable description of the magnitude of the hydrophobic attraction for later analysis, and does not imply that the hydrophobic forces are a form of vdW interaction. Both here and in the case of bare mica surfaces across conductivity water [17] the surfaces are rigidly coupled once jump into contact has occurred, whereas prior to adhesive contact any

[6] The theoretical vdW force expected between two crossed cylinders of radius of curvature R, at closest distance D, is $F_n(D) = -AR/6D^2$, where A is the Hamaker constant. The condition for a jump-in is thus $\mathrm{d}F/\mathrm{d}D = AR/3D^3 > K_n = 150$ N m. For two hydrophobic-coated mica surfaces across water $A = 1.5 \times 10^{-20}$ J, yielding $D_j < (AR/3K_n)^{1/3} \sim 7$ nm (for $R \sim 1$ cm). In order to use this expression to account for $D_j = 11 \pm 2$ nm we need to assume an effective Hamaker constant of $A_{eff} > 3D_j^3K_n/R = 10^{-19}$ J.

shear stress across the sheared intervening aqueous films—over the range of shear rates used (300–600 s^{-1})—was below our resolution at any film thickness.

4. Analysis of the jump time and discussion

The viscosity of the water when it is confined to sub-nanometre films ($D < 2$–3 nm), down to the final few ångstroms, may be evaluated by considering in detail the processes occurring as the surfaces jump from $D = D_j$ (or D_j^{STAI}) to adhesive contact. In this regime, treating the effective geometry of the curved surfaces as that of a sphere, radius R, approaching a flat surface, the equation of motion is to a good approximation

$$M(\mathrm{d}^2D/\mathrm{d}t^2) + 6\pi R^2\eta_{eff}[(\mathrm{d}D/\mathrm{d}t)/D]f^* = F_{\mathrm{vdW}}(D) - K_n(D_j - D) \tag{1}$$

where M is the effective mass of the moving mica surface and its mounting; the second term on the left is the Reynolds hydrodynamic resistance force [38] to approach of a sphere to a flat across a medium of effective viscosity η_{eff}, where f^* is the correction factor to account for slippage of liquid at the surface [18]. For two similar hydrophobic surfaces,

$$f^* = D/3b[(1 + D/6b)\ln(1 + 6b/D) - 1] \tag{2}$$

where b is the so-called slip length, which characterizes the extent of liquid flow near the surface. This is the distance behind the liquid/solid interface at which the liquid velocity extrapolates to zero [39]. This model is accurate for low Reynolds numbers and for small surface separations ($D < R$). Both these approximations are valid for our measurements. In our earlier treatment [17] $f^* = 1$ was used, reflecting the assumption that no slip occurs at the hydrophilic mica surfaces. In this surface separation regime the force driving the approach of the hydrophilic surfaces is given by the vdW dispersive attraction, $F_{\mathrm{vdW}}(D) = AR/6D^2$, where A is the relevant Hamaker constant ($A = 2 \times 10^{-20}$ J), or for the case of hydrophobic surfaces by a similar expression (see earlier), where $A = A_{eff} = 10^{-19}$ J is used to account for the total attractive hydrophobic interaction. We ignore the very small change in the double-layer interaction in the interval $\{D_j, D_0\}$ or $\{D_j^{STAI}, D_0^{STAI}\}$. It is readily shown that in the conditions of our experiments the inertial term and that (in K_n) due to the spring bending are negligible compared with the others, yielding, after some algebra, the time τ_j for the surfaces to jump from D_j to D_0 (or D_j^{STAI} to D_0^{STAI}):

$$\begin{aligned}\tau_j(D_j, D_0, \eta_{eff}) &= \int_{D_0}^{D_j} (36\pi R\eta_{eff} Df^*/A)\,\mathrm{d}D \\ &= \pi R\eta_{eff}\{-6b(D_j - D_0)[12b^2 + D_j^2 + D_jD_0 + D_0^2 - b(D_j + D_0)] \\ &\quad + D_j^3(8b + D_j)\ln(1 + 6b/D_j) + 432b^4\ln[(6b + D_j)/(6b + D_0)] \\ &\quad - D_0^3(8b + D_0)\ln(1 + 6b/D_0)\}/2Ab^2.\end{aligned} \tag{3}$$

The variation of τ_j with D_j is shown in figure 3, using $\eta_{eff} = \eta_{bulk} = 0.86 \times 10^{-3}$ Pa s, the viscosity of bulk water at 23 °C. The main figure shows the case of hydrophobic surfaces (substituting in equation (3) D_0^{STAI} and D_j^{STAI}), for different b (slip length) values in the range up to 100 nm. A typical b value for water flowing past hydrophobic surfaces is about 10 nm [18, 19, 40]; 100 nm may be viewed as an upper limit on b as it is significantly higher than reported experimental b values for water on hydrophobic surfaces similar to the STAI, even at very high flow rates (i.e. $\mathrm{d}D/\mathrm{d}t$, t denotes time) [18, 19]. The inset shows the variation of τ_j with D_j for b in the range up to 10 nm, in the case of hydrophilic surfaces, where non-slip boundary conditions are usually assumed [18].

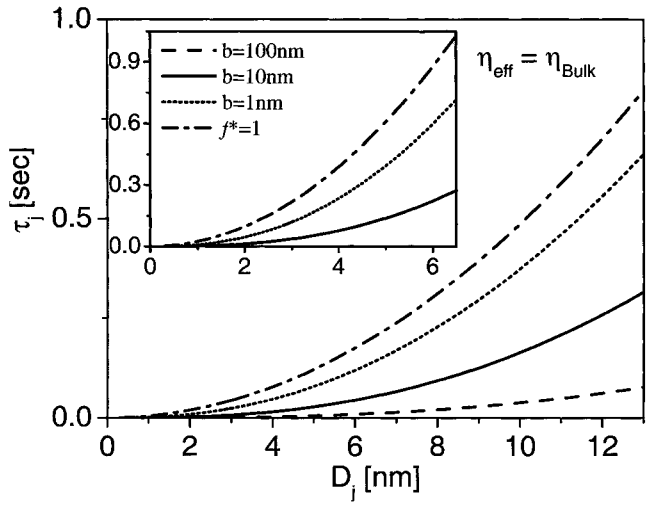

Figure 3. The main figure shows how, for an effective viscosity $\eta_{eff} = \eta_{bulk} = 0.86$ mPa s (the viscosity of bulk water at 23 °C), the jump time τ_j is expected to vary with the jump distance D_j according to equation (3), for the case of hydrophobic surfaces ($A = A_{eff} = 10^{-19}$ J) and different values of slip length b—up to 100 nm. The inset shows the behaviour in the case of hydrophilic mica surfaces ($A = 2 \times 10^{-20}$ J); slip lengths at such interfaces are generally assumed to be zero or very small, hence only b values up to 10 nm are shown in the inset. D_0 was taken as 0.3 nm for hydrophilic surfaces and 0.7 nm for hydrophobic surfaces, though variations of ± 0.3 nm in D_0 do not significantly change the calculated curves.

In figure 4 the implicit relation (from equation (3)) between the jump time to contact τ_j and the effective viscosity η_{eff} is shown, for different values of b. The main figure shows the case of hydrophobic surfaces where b is in the range up to 100 nm and the jump separation is $D_j^{STAI} = 11 \pm 2$ nm, whereas the inset shows the case of hydrophilic surfaces for which $D_j = 3.5 \pm 1$ nm. In each case the upper limit on η_{eff} is given by the combination of the shortest jump distance, highest b and longest τ_j. This shows that the viscosity of water confined between hydrophobic surfaces to films of thickness in the range 11 ± 2 nm down to contact, as determined from our experimental jump times and the above analysis, is within a factor about 10–20 *at most* of the viscosity of bulk water η_{bulk} (arrow). Similarly, the viscosity of water confined between hydrophilic surfaces to gaps in the range 3.5 ± 1 nm down to contact is within a factor 20 or so at most of η_{bulk}, though this upper limit involves assumption of a non-realistic slip length of 10 nm at the hydrophilic surface. A more detailed consideration (to be published) shows that the magnitude of η_{eff} remains within this range at all film thicknesses throughout the jump into contact. The relatively high η_{eff} values arise from the high upper limit on b. More realistic b values (up to 1 nm and about 10 nm for hydrophilic and hydrophobic surfaces, respectively), applicable to our approach rates [19] (about 30 nm s^{-1}), would have yielded an upper limit of η_{eff} much closer to η_{bulk} (see figure 4), as demonstrated earlier [17] for the case of hydrophilic surfaces.

We note that the effective maximal shear rates during our measurements vary from about 10^1–10^2 s^{-1} prior to the jump-in due to ambient vibration [17] to about 10^4 s^{-1} during the jump-in itself (at separation of 0.5 nm from contact) [41]. Within our resolution the effective viscosity of the confined water is similar at these different shear rates, suggesting that its behaviour is Newtonian within this range.

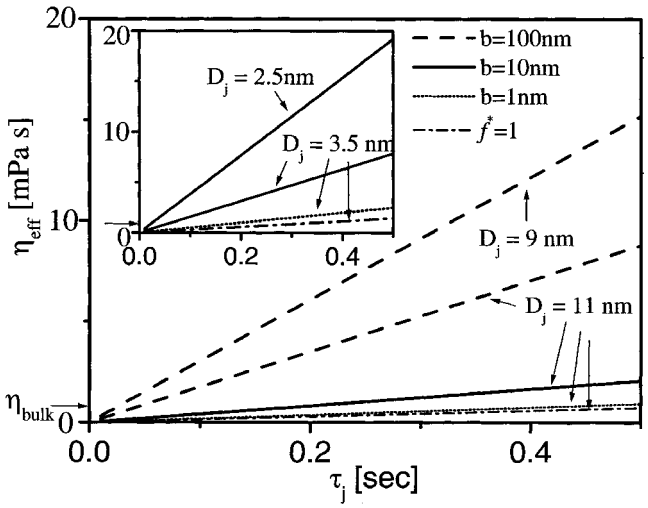

Figure 4. The main figure shows the effective viscosity η_{eff} of the liquid being squeezed out of the hydrophobic gap corresponding to the experimentally determined jump time to contact τ_j (0.5 s or less), for different values of slip length b, using $A = A_{eff} = 10^{-19}$ J and for $D_j = 11$ nm. The upper dashed line corresponds to $b = 100$ nm and $D_j = 9$ nm, and sets the upper limit on η_{eff}, within our scatter. The inset shows the behaviour for the case of hydrophilic surfaces ($A = 2 \times 10^{-20}$ J) and $D_j = 3.5$ nm. The upper solid line corresponds to $b = 10$ nm and $D_j = 2.5$ nm and sets an upper limit on η_{eff}. The viscosity of bulk water at 23 °C, η_{bulk}, is indicated with arrows. D_0 values as in figure 3.

These results represent a direct evaluation of the viscosity of water confined to sub-nanometre films between hydrophobic and hydrophilic surfaces, taking into account both slip and no-slip boundary conditions. The similar upper limits on η_{eff} exhibited by two completely different surfaces suggests the origin of these observations is related to the unique properties of water rather than the nature of the confining surfaces. The main reason for this, as has been discussed elsewhere [17], is that the confining surfaces suppress the formation of the highly directional hydrogen bond network required for freezing of water. Including a finite slip length as the slip boundary condition, in both cases, did not significantly influence the essence of our results [17], which is that the viscosity of highly confined water remains comparable to its bulk value. This persistent fluidity clearly has interesting consequences for many phenomena where confined water is implicated. It should be emphasized however that our present study examined highly purified, salt-free water, where the ion concentration (of order 10^{-6} M) is lower by many orders of magnitude than is commonly found in nature or technology.

5. Conclusions

The viscosity of water confined to nanometre and subnanometre films has been evaluated based on an analysis of the experimentally measured jump time to contact of both hydrophilic and hydrophobic confining surfaces. A previous study [17], using stick boundary conditions appropriate to a hydrophilic surface and a vdW attraction between the surfaces, demonstrated that the viscosity of the water was close to its bulk value even when confined to films in the thickness range 3.5–0 $\pm$ 0.4 nm. The present work reveals two new features: if an arbitrary slip (within an appropriate range) is incorporated into the previous analysis for the confining *hydrophilic* surfaces, the viscosity determined for the confined water still remains comparable

to its bulk value. For the case of two confining hydrophobic surfaces, the analysis must be modified to take account of the stronger hydrophobic forces pulling the surfaces into contact, and also to take due account of larger slip at the solid–liquid interface. Over the range of parameters measured, we have found that in this second case (confining *hydrophobic* surfaces) the effective viscosity of the water in films down to the subnanometre range also remains comparable to its bulk value.

Acknowledgments

We thank R Tadmor for advice on the STAI coating procedure. We thank the Eshkol Foundation (UR), the NSERC (Natural Sciences and Engineering Research Council of Canada) and Charpak-Vered Fund (SG), the US–Israel Binational Science Foundation, the Deutsche-Israelische Program (DIP) and the Minerva Foundation for their support of this work. This paper is an adaptation of a talk given at Les Houches on the most enjoyable occasion of Jean-Pierre Hansen's 60th Birthday: Happy Birthday, Jean-Pierre!

References

[1] See 'The hydration problem in solution biophysics' in a special issue of 2001 *Biophys. Chem.* **93** 87–244 and papers therein
[2] Bellissent-Funel M C, Lal J and Bosio L 1993 *J. Chem. Phys.* **98** 4246–52
[3] Bellissent-Funel M-C, Chen S H and Zanotti J M 1995 *Phys. Rev.* E **51** 4558
[4] Chen S-H and Bellissent-Funel M-C 1994 *Hydrogen Bond Networks* vol 435, ed M-C Bellissent-Funel and J C Dore (Dordrecht: Kluwer) pp 307–36
[5] Clifford J 1975 *Water in Disperse Systems* vol 5, ed F Franks (New York: Plenum) pp 75–132
[6] Israelachvili J N and Wennerstrom H 1996 *Nature* **379** 219–25
[7] Pissis P, Laudat J, Daoukaki-Diamanti D and Kyritsis A 1994 *Hydrogen Bond Networks* vol 435, ed M-C Bellissent-Funel and J C Dore (Dordrecht: Kluwer) pp 425–32
[8] Ricci M A *et al* 2000 *J. Phys.: Condens. Matter* **12** A345–50
[9] Rossky P J 1994 *Hydrogen Bond Networks* vol 435, ed M-C Bellissent-Funel and J C Dore (Dordrecht: Kluwer) pp 337–8
[10] Xia X, Perera L, Essmann U and Berkowitz M L 1995 *Surf. Sci.* **335** 401–15
[11] Meyer M and Stanley H E 1999 *J. Phys. Chem.* B **103** 9728–30
[12] Gallo P *et al* 2000 *Europhys. Lett.* **49** 183–8
[13] Israelachvili J N 1986 *J. Colloid Interface Sci.* **110** 263–71
[14] Horn R G, Smith D T and Haller W 1989 *Chem. Phys. Lett.* **162** 404–8
[15] Klein J and Kumacheva E 1995 *Science* **269** 816–19
[16] Israelachvili J N and McGuiggan P M 1988 *Science* **240** 189–91
[17] Raviv U, Laurat P and Klein J 2001 *Nature* **413** 51–4
[18] Vinogradova O I 1995 *Langmuir* **11** 2213–20
[19] Craig V S J, Neto C and Williams D R M 2001 *Phys. Rev. Lett.* **87** 054504-1–4
[20] Baudry J, Charlaix E, Tonck A and Mazuyer D 2001 *Langmuir* **17** 5232–6
[21] Pit R, Hervet H and Leger L 2000 *Phys. Rev. Lett.* **85** 980–83
[22] Klein J and Kumacheva E 1998 *J. Chem. Phys.* **108** 6996–7009
[23] Klein J 1983 *J. Chem. Soc., Faraday Trans.* I **79** 99–118
[24] Kodawa *et al* 1990 *J. Phys. Chem.* **94** 815
[25] Tadmor R, Rosensweig R E, Frey J and Klein J 2000 *Langmuir* **16** 9117–20
[26] Pashley R M 1981 *J. Colloid Interface Sci.* **80** 153–62
[27] Raviv U *et al* 2002 at press
[28] Pashley R M 1981 *J. Colloid Interface Sci.* **83** 531–46
[29] Pashley R M and Israelachvili J N 1981 *Colloids Surf.* **2** 169–87
[30] Cleasson P M, Blom C E, Herder P C and Ninham B W 1986 *J. Colloid Interface Sci.* **114** 234
[31] Abraham T, Giasson S, Gohy J F and Jerome R 2000 *Langmuir* **16** 4286–92
[32] Abraham T *et al* 2000 *Macromolecules* **33** 6051–9
[33] Giasson S, Kuhl T L and Israelachvili J N 1998 *Langmuir* **14** 891–8

[34] Pugh R J 1991 *Int. J. Miner. Process.* **33** 307
[35] Wood J and Sharma R 1995 *Langmuir* **11** 4797–802
[36] Christenson H K and Claesson P M 2001 *Adv. Colloid Interface Sci.* **91** 391–436
[37] Raviv U, Laurat P and Klein J 2002 *J. Chem. Phys.* **116** 5167–72
[38] Happel J and Brenner H 1965 *Low Reynolds Numbers Hydrodynamics* (Englewood Cliffs, NJ: Prentice-Hall)
[39] Brochard F and de Gennes P G 1992 *Langmuir* **8** 3033
[40] Churaev N V, Sobolev V D and Somov A N 1984 *J. Colloid Interface Sci.* **97** 574
[41] Chan D Y C and R G Horn 1985 *J. Chem. Phys.* **83** 5311–24